

# Linear models for control of cavity flow oscillations

By CLARENCE W. ROWLEY<sup>1</sup>, DAVID R. WILLIAMS<sup>2</sup>,  
TIM COLONIUS<sup>3</sup>, RICHARD M. MURRAY<sup>3</sup>, AND  
DOUGLAS G. MACMARTIN<sup>3</sup>

<sup>1</sup>Mechanical and Aerospace Engineering, Princeton University, Princeton, NJ 08544, USA

<sup>2</sup>Mechanical, Materials, and Aerospace Engineering, Illinois Institute of Technology, Chicago, IL 60616, USA

<sup>3</sup>Mechanical Engineering, California Institute of Technology, Pasadena, CA 91125, USA

(Received ?? and in revised form ??)

Models for understanding and controlling oscillations in the flow past a rectangular cavity are developed. These models may be used to guide control designs, to understand performance limits of feedback, and to better understand experimental results. Traditionally, cavity oscillations are assumed to be *self-sustained*: no external disturbances are necessary to maintain the oscillations, and amplitudes are limited by nonlinearities. We present experimental data which suggests that in some regimes, the oscillations may not be self-sustained, but rather *lightly damped*: oscillations are sustained by external forcing, such as boundary layer turbulence. In these regimes, linear models suffice to describe the behavior, and the final amplitude of oscillations depends on the characteristics of the external disturbances. These linear models are particularly appropriate for describing cavities in which feedback has been used for noise suppression, as the oscillations are small and nonlinearities are less likely to be important.

---

## 1. Introduction

Recent experiments using feedback to control cavity oscillations have met with limited success. Some early flow control experiments (Cattafesta *et al.* 1999; Williams *et al.* 2000) suppressed individual Rossiter tones by up to 20dB with active feedback; however, other tones were unaffected or enhanced by the control system. When the control gains were increased to achieve greater suppression, new frequencies would appear in the spectrum, or the suppressed peak would split. These effects were undesirable, and unpredictable. The goal of this paper is to use physics-based models to understand these effects, guide future control designs, and understand any fundamental performance limits, for a given choice of sensor and actuator.

The usual description of cavity oscillations involves *self-sustained oscillations*, caused by the familiar Rossiter mechanism (Rossiter 1964; Tam & Block 1978; Rowley *et al.* 2002): small disturbances are amplified by the shear layer, and produce acoustic waves when they impinge on the downstream corner; these acoustic waves then propagate upstream and excite further instabilities in the shear layer, leading to self-forcing. In the absence of any external forcing, the cavity would continue to oscillate. The cavity behaves as a dynamical system with an stable limit cycle about an *unstable* equilibrium point (a steady solution of Navier-Stokes). The amplitude of the oscillations is determined by nonlinearities, such as saturation of instabilities in the shear layer.

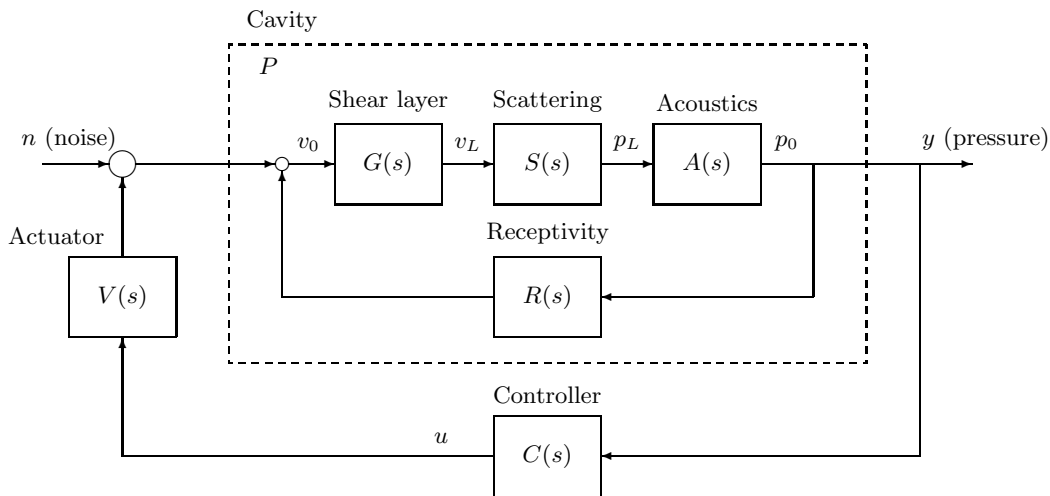


FIGURE 1. Block diagram of cavity model.

By contrast, we demonstrate that for many conditions where oscillations are observed, the cavity behaves as a *stable*, lightly damped system. The flow amplifies noise at certain resonant frequencies, but if the external forcing were removed, the oscillations would disappear. Purely linear models may be used to describe this mechanism, as the final amplitude of oscillations is determined by the amplitude of the forcing disturbances (e.g., boundary layer turbulence, or wall roughness), and by the linear gain of the system. Nonlinearities, such as saturation of instability waves in the shear layer, may still be present in this mechanism, and will also affect the final amplitude of oscillations, but they are not necessary to explain finite-amplitude oscillations. We show that the previously noted performance limitations of feedback control are explained by this alternative view of cavity oscillations, and that controllers can be designed to minimize the adverse effects.

The paper is organized as follows: we present the physics-based linear model in section 2, then describe some experimental results in section 3. In section 4 we use the model to explain a peak-splitting phenomenon observed in the experiment, and to understand some fundamental limitations of any feedback controller used to suppress the oscillations.

## 2. Analytical model

The cavity dynamics are modeled after the familiar Rossiter mechanism described in the introduction. A block diagram of the model is shown in Figure 1, where we represent each component of the physical mechanism as a separate transfer function. Here,  $G(s)$  represents the shear-layer transfer function, i.e., the transfer function from velocity disturbances  $v_0$  at the leading edge to velocity disturbances  $v_L$  at the trailing edge. Transfer functions for acoustic scattering, propagation, and receptivity are given by  $S$ ,  $A$ , and  $R$ , and in the diagram  $p_0$  and  $p_L$  denote pressure disturbances at the leading and trailing edges, respectively.

The other transfer functions depicted in Figure 1 represent the influence of controller and an actuator (for instance, a jet or oscillating flap at the cavity leading edge). The controller transfer function, which we choose, is given by  $C(s)$ , and the actuator dynamics are described by a transfer function  $V(s)$ . In this diagram, the output  $y$  is the pressure at the upstream lip of the cavity, which in an experiment may be measured by

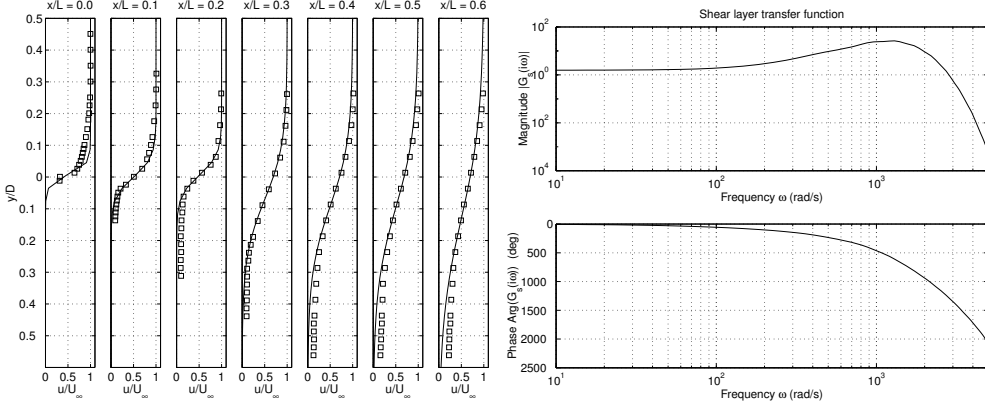


FIGURE 2. *Left*: velocity profiles for the cavity shear layer. Hot wire measurements ( $\square$ ) and tanh profiles with same vorticity thickness and deflection (—). *Right*: Bode plot of shear layer transfer function  $G_s(s)$ , determined from linear stability theory.

a pressure transducer. The plant is excited by external noise (e.g., turbulent boundary layer fluctuations), modeled by an input disturbance  $n$ .

The overall transfer function for the cavity is then

$$P(s) = \frac{ASG}{1 - RASG}. \quad (2.1)$$

For the purposes of studying the dynamical features of this model, we ignore the actuator dynamics, setting  $V(s) = 1$ . (These actuator dynamics may in principle be measured from the experiment, and once measured, their effects may be inverted out of the control laws we obtain.) Theoretical models for the remaining transfer functions are discussed below.

### 2.1. Shear layer

The shear layer transfer function  $G(s)$  may be determined from linear stability theory. We begin with velocity profiles measured in experiments by Williams *et al.* (2000), shown in Figure 2. These profiles are from an experiment with Mach number  $M = 0.35$ , in a cavity with aspect ratio  $L/D = 5$ . Figure 2 shows the experimental data along with hyperbolic tangent profiles with the same vorticity thickness. The spreading rate of the shear layer is determined from a linear fit to the data, and used as an input to a linear stability calculation to determine the amplification and phase of shear layer disturbances. We then fit a rational function to the resulting transfer function (with little loss of accuracy), and the result is shown in Figure 2. Using this rational function approximation, one may immediately obtain a state-space realization of the transfer function, and apply standard tools from control theory to the resulting model.

As a simpler alternative, we also consider the shear layer modeled as a second-order system with a time delay

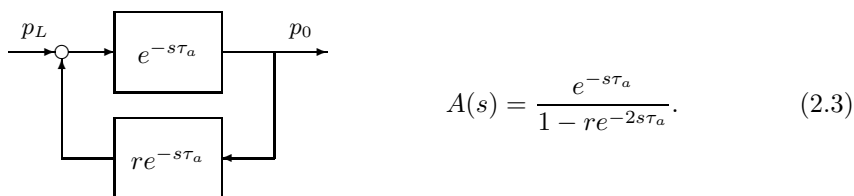
$$G(s) = G_0(s)e^{-s\tau_s} = \frac{\omega_0^2}{s^2 + 2\zeta\omega_0s + \omega_0^2} e^{-s\tau_s}, \quad (2.2)$$

where  $\omega_0$  is the natural frequency of the second-order system (e.g., this may be chosen to be the frequency of the most unstable Kelvin-Helmholtz mode), and  $\zeta$  is the damping, related to the maximum amplification. The time delay  $\tau_s$  is the convection time for a disturbance to travel the length of the cavity, and is given by  $\tau_s = L/c_p$ , where  $c_p$  is the mean phase speed.

The purpose of the second-order model (2.2) is not to perfectly fit the linear stability results, but rather to provide a simple model that captures the same general features: amplification at low frequencies, attenuation at high frequencies, with an appropriate phase delay. In addition, its adjustable parameters allow the model to be tuned to match specific experimental results, and give insight into the effects of the various parameters. Note that for control, one needs the model to be accurate only in the frequency range over which the controller acts, and this model may be tuned to arbitrarily high accuracy in a narrower range of frequencies.

### 2.2. Acoustics

The model we use for acoustic propagation in the cavity consists of a simple time-delay, with reflection:



Here,  $\tau_a = L/a$  is a time delay which represents the acoustic lag between the trailing edge and leading edge (here,  $L$  is the cavity length and  $a$  is the sound speed inside the cavity). An acoustic wave emanating from the downstream corner  $x = L$  propagates upstream, and some of it reflects off the upstream wall, propagates downstream, and again reflects off the downstream wall. The reflection coefficient  $r$  measures the total efficiency of the reflection process, including losses via acoustic radiation to the farfield (e.g., if both reflections are perfect, with no radiation to the farfield, then  $r = 1$ ; if each reflection reduces the amplitude by 0.5, then  $r = 0.25$ ). This model therefore captures longitudinal modes of acoustic resonance, but ignores transverse modes. For  $r = 0$ , the model is a pure time delay, and for  $0 < r < 1$ , the Bode magnitude plot of  $A(s)$  shows resonant peaks at the fundamental frequency  $1/(2\tau_a)$  and its harmonics. Note that these acoustic resonances are not the Rossiter frequencies, but they may influence the mode selection, determining which Rossiter mode is dominant, as described in Williams *et al.* (2000).

### 2.3. Scattering and Receptivity

Scattering and receptivity effects at the trailing and leading edge, respectively, are the least simple to model. They have been studied by Crighton (1992) for edge tones, and Kerschen & Tumin (2003) for cavity flows. In Rossiter's empirical formula for predicting cavity frequencies, the scattering and receptivity effects are treated together as a simple phase lag, independent of frequency. Here, we follow Rossiter's approach and model scattering and receptivity each as constant gains. This approximation is justified since the strongest frequency dependence of the amplitude occurs in the shear layer (Kelvin-Helmholtz instability), and the strongest frequency dependence of the phase results from time delays in the shear layer and acoustics, as discussed above. For a more accurate model, the scattering and receptivity results of Kerschen & Tumin (2003) could be employed.

### 2.4. Overall cavity model

The overall cavity transfer function  $P$  is formed from equation (2.1). To gain some insight into the model, first we consider some special cases. In particular, for certain choices of

parameters, we recover the Rossiter formula for the frequencies of oscillation. For the shear layer model (2.2), suppose  $G_0(s) = e^{-i2\pi\gamma}$ , a constant phase, and take  $\tau_s = L/c_p$ , with  $c_p/U = \kappa$ . Assuming no reflections ( $r = 0$ ) in the acoustic model (2.3), the overall transfer function becomes

$$P(s) = \frac{e^{-i2\pi\gamma}e^{-s\tau_s}}{1 - e^{-i2\pi\gamma}e^{-s(\tau_s+\tau_a)}}$$

which has poles at  $s = i\omega$ , with

$$\frac{\omega L}{2\pi U} = \frac{n - \gamma}{M + 1/\kappa}, \quad n = 1, 2, \dots, \quad (2.4)$$

which is the familiar Rossiter formula for the frequencies of oscillation. The other features of the model include the effects of longitudinal acoustic modes in the cavity (with  $r > 0$ ), as well as amplification effects by the shear layer (with  $G_0(i\omega) \neq \text{const}$ ). Note that both of these features primarily affect the *amplitude* of the loop gain, and hence the stability of each mode, and have only a minor effect (due to their phase) on the overall resonant frequencies.

The advantage of the present model over Rossiter’s original formula is, of course, that the present model is *dynamically accurate*: it does not merely predict resonant frequencies, but predicts how the output (a pressure measurement) evolves in time, given an arbitrary actuator input or external disturbance. We will use these models to explain some features in the experiment described in the next section.

### 3. Experimental dynamics

Experiments were performed using the 3 ft  $\times$  3 ft subsonic wind tunnel at the United States Air Force Academy in Colorado Springs. A cavity model 20 in long, 4 in deep, and 15 in wide was installed in the floor of the test section, and a diagram of the setup is shown in Figure 3.

The cavity was instrumented with eight Kulite pressure transducers placed along the cavity walls, one on the upstream wall, one on the downstream wall, and six along the floor, approximately equally spaced. All signals were passed through anti-aliasing filters prior to sampling by a digital data acquisition system at 6 kHz.

The flow was forced using zero-net-mass blowing through a slot in the upstream wall of the cavity, shown in Figure 3. The actuator was a pair of 500-Watt 8 in diameter loudspeakers in an enclosed chamber. Though the actuator injects zero net mass through the slot, a nonzero net momentum is induced by spanwise vortices generated by periodically blowing through the slot (the “synthetic jet” effect (Smith & Glezer 1998)).

In order to suppress oscillations, both analog and digital controllers were implemented. The analog controller consisted of a bandpass filter and a phase shifter. Digital controllers were implemented using a dSPACE interface board, running on a separate computer from the data acquisition system. For typical controllers we used, the maximum sample rate was about 20 kHz.

#### 3.1. Lightly damped vs. self-sustained oscillations

As mentioned in the introduction, two possible mechanisms may lead to finite-amplitude oscillations. The conventional view, as in Tam & Block (1978) and Rowley *et al.* (2002), is that the oscillations are *self-sustained*: in this mechanism, the linearized system (about a steady solution of Navier-Stokes) is unstable, so tiny perturbations will grow in time, and eventually saturate once nonlinearities become important. An alternative view, considered recently for combustion instabilities by Banaszuk *et al.* (2001), is that the system

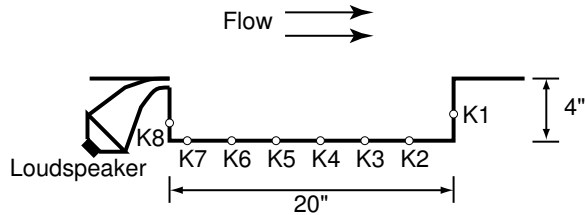


FIGURE 3. Diagram of experimental apparatus (side view). Location of Kulite pressure transducers is indicated by K1–K8.

is linearly stable, but *lightly damped*, and constantly excited by external disturbances. These disturbances are then amplified, causing oscillations at the resonant frequency of the plant, but if the disturbances were removed, the oscillations would also disappear. In practice, disturbances such as boundary layer turbulence and wall roughness are always present, so this mechanism can also explain persistent oscillations. In this mechanism, nonlinearities may not be important: the amplitude of the oscillations is determined by the amplitude of the excitation noise, and though nonlinearities may still be present, they are not necessary to explain finite-amplitude oscillations. In this section, we demonstrate that the cavity may operate in either the lightly-damped or self-sustained regime, depending on the Mach number and other parameters.

Note that in both cases mentioned above, the shear layer is locally convectively unstable (i.e., not absolutely unstable), using the terminology of Huerre & Monkewitz (1990). However, the flow may still be globally unstable if the acoustic feedback provides a loop gain that is greater than unity. As discussed in Rowley *et al.* (2002), several parameters affect this loop gain, including thickness of the upstream boundary layer, and shear layer spreading rate, which is influenced by the incident turbulence level (Sarohia 1975). Note that the conditions classified as “no oscillations” in the numerical investigations in Rowley *et al.* (2002) may still exhibit oscillations in an experiment, where noise is present.

Stable and unstable regimes may not be unambiguously identified using only frequency spectra. Both regimes are characterized by peaks at the resonant frequencies, and one cannot tell whether the system is in a (noisy) limit cycle, or whether it is stable, merely amplifying disturbances at certain frequencies. However, it is possible to distinguish between the two regimes using the probability density function (PDF) of the output signal (Mezić & Banaszuk 2000).

If the input disturbances have a Gaussian distribution, the PDF of the stable system excited by these disturbances will also be Gaussian. By contrast, the PDF of a limit cycling system (say  $y(t) = \sin(t)$ ) will have two peaks, because the system spends more time near the extrema of the limit cycle. In addition, the phase portrait of a limit cycling system will be a closed curve (or, with noise, a “fuzzy” closed curve), while the phase portrait of a stable system forced by noise will be concentrated about a point.

Measurements from the cavity experiment at two different Mach numbers are shown in Figure 4. At  $M = 0.34$ , the system appears to be unstable, in a limit cycle. The phase portrait indeed looks like a fuzzy ellipse, and the PDF has two distinct peaks. However, at  $M = 0.45$ , the system appears to be stable, driven by noise. The phase portrait is concentrated about a point, and the PDF has a single peak which closely resembles a Gaussian.

A sweep of Mach numbers from 0.1 to 0.45 revealed that  $M = 0.34$  is the only Mach number where the unstable regime is observed. Furthermore, at this Mach number, only

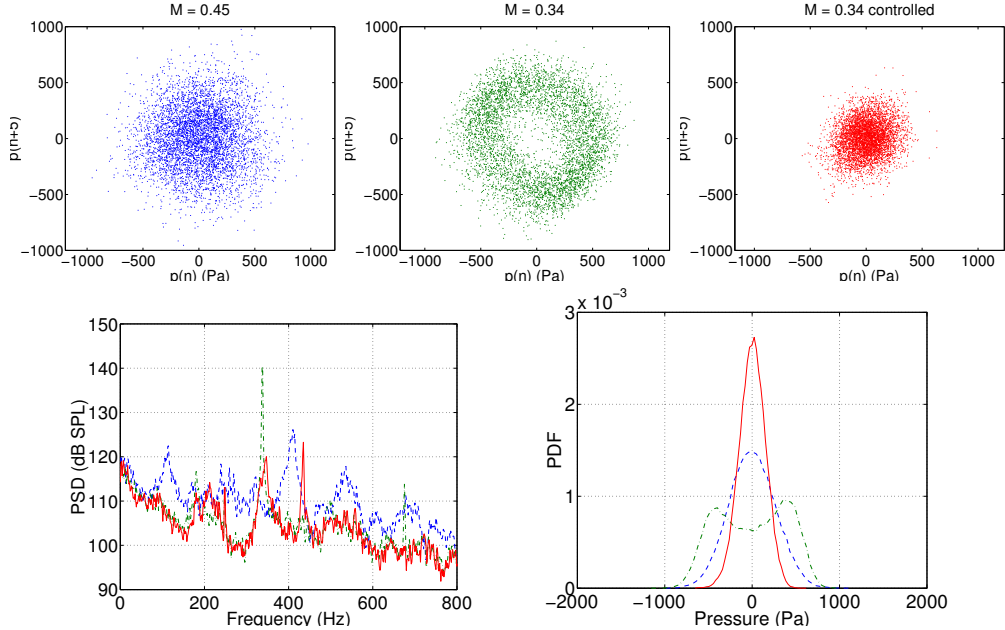


FIGURE 4. Top row: phase portraits of pressure signal from Kulite 7 at Mach numbers  $M = 0.45$  (left),  $M = 0.34$  (center); and at  $M = 0.34$  with feedback controller tuned to suppress oscillations (right). Bottom row: spectra (left) and PDFs for the three datasets:  $M = 0.45$  (-----),  $M = 0.34$  unforced (— · —), and  $M = 0.34$  with control (——). The  $M = 0.34$  case is in a limit cycle, but for the other cases, amplification of external disturbances is the dominant oscillation mechanism.

a single frequency is observed, while at most other Mach numbers, multiple modes exist simultaneously. This is probably because at  $M = 0.34$ , the longitudinal acoustic modes in the cavity reinforce the Rossiter modes: the frequency of the first longitudinal mode coincides with the frequency of the third Rossiter mode (Williams *et al.* 2000). Presumably, this reinforcement increases the loop gain at this frequency enough to cause the system ( $P$  in Figure 1) to become unstable.

We note that more generally, any effect which increases this loop gain may cause instability. In particular, Rowley *et al.* (2002) observed that cavities with laminar upstream boundary layers will experience greater shear-layer amplification, and thus a greater loop gain. This is further corroborated by Sarohia (1975), who observed that cavities with laminar upstream boundary layers were more likely to exhibit oscillations. An explanation for this, given in Rowley *et al.* (2002), is that laminar boundary layers lead to greater shear layer amplification, which leads to a greater overall loop gain. This may explain why the simulations in Rowley *et al.* (2002) with laminar upstream boundary layers are apparently in the unstable regime, where the parameter values are otherwise similar to those in the present experiment.

### 3.2. Behavior with and without active suppression

The oscillations were suppressed using an analog controller consisting of a bandpass filter and a phase shifter, used in previous experiments by Williams *et al.* (2000), and pressure measurements for the baseline and controlled cases are compared in Figure 4. From the phase portrait and the PDF, it appears that the unforced case is limit cycling, but with control the system is stable. The frequency response shows that the closed-loop system does excite oscillations at a new frequency (about 420 Hz), and we discuss these adverse

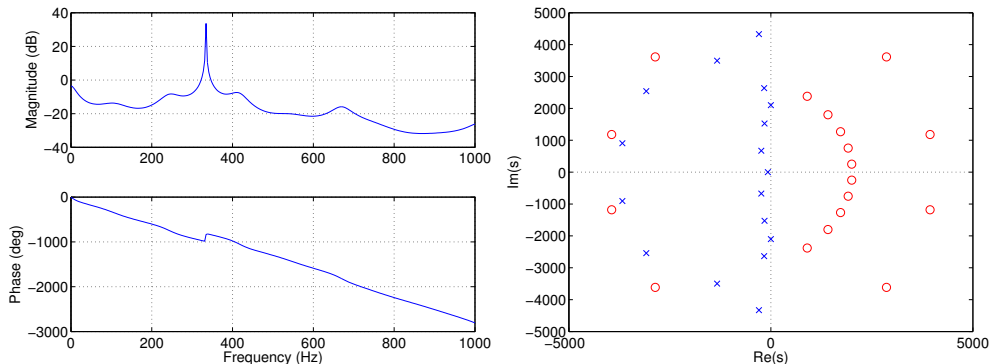


FIGURE 5. Left: Magnitude and phase of  $P(i\omega)$  for cavity model at  $M = 0.34$ ; Right: poles ( $\times$ ) and zeros ( $\circ$ ) of  $P(s)$  at  $M = 0.34$ , with Padé approximations for the time delays.

effects of control later, but from the PDF it appears that these oscillations are the result of disturbance amplification, not instability.

#### 4. Performance limits

In this section, we use the analytical model developed in section 2 to understand any fundamental limitations of feedback control, for the given arrangement of sensors and actuators.

##### 4.1. Empirically tuned model

The model we use is given by equation (2.1), with parameters chosen to make the model approximately agree with the experimental conditions at  $M = 0.35$ , and the resulting frequency response is shown in Figure 5. For the shear layer, equation (2.2) is used, with  $\omega_0 = 350$  Hz,  $\zeta = .2$ , and  $\tau_s = L/c_p$ , with  $\kappa = c_p/U = 0.625$ . (Here,  $U \approx 117.5$  m/s is the freestream velocity.) For the time delay, we use an 8th-order Padé approximation to obtain a rational transfer function. The acoustics are modeled by equation (2.3) with  $r = 0.1$  and  $\tau_a = L/a$ , where  $a$  is the sound speed in the freestream, and a 6th-order Padé approximation is used for the time delay. Variations in the sound speed are assumed small for this relatively low Mach number. The scattering gain is taken to be 0.2, and changing this parameter adjusts the stability of the system: for larger values of this gain, the system becomes unstable, and for smaller values, the system is more heavily damped.

For the model shown in Figure 5, the magnitude of the frequency response may be viewed precisely as the amount the flow amplifies disturbances at each frequency. The peaks predicted by the model (imaginary parts of the lightly-damped poles) are at 114 Hz, 234 Hz, and 336 Hz, which correspond to the first three Rossiter frequencies. The third peak is the strongest because the shear layer amplification is the greatest for this frequency, and because the cavity acoustics reinforce oscillations at this frequency.

##### 4.2. Peak-splitting phenomenon

In the spectra shown in Figure 4, the controller is able to reduce the amplitude of the tone at 340 Hz, but not eliminate it completely. Increasing the controller’s gain does not result in further suppression, as shown in Figure 6, which shows spectra from three different controllers with a larger gain than that shown in Figure 4. These controllers were implemented digitally, but had the same structure as the analog controller used in

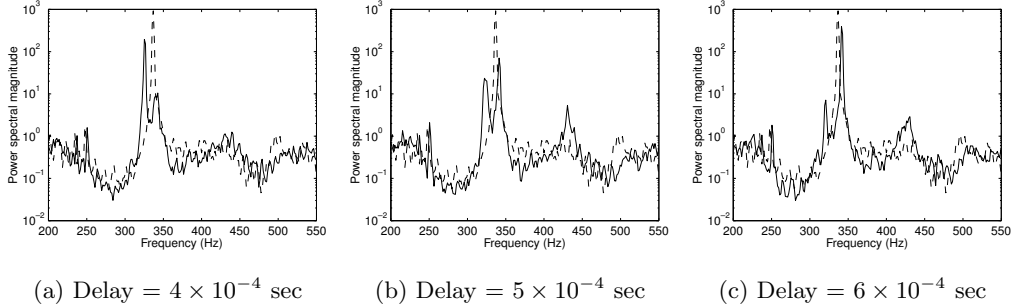


FIGURE 6. Power spectra with digital controllers, showing sidebands: control off (----); control on (—).

Figure 4: a 2nd-order Butterworth filter with a passband of 290–390 Hz was used, along with a time delay, which was varied as shown in Figure 6.

In Figure 6, the main resonant frequency at 337 Hz is almost completely attenuated, but sidebands appear very close in frequency, at about 320 Hz and 341 Hz. As the time delay is changed, the relative strength of the sidebands changes, and the frequency changes slightly—the lower frequency shifts from 320 to 325 Hz in Figures (a)–(c). In retrospect, this peak-splitting phenomenon also appears in some previous closed-loop cavity experiments (e.g., Cattafesta *et al.* (1999), Fig. 5). This phenomenon has also been observed in combustion experiments at UTRC by Banaszuk *et al.* (2001), where they have been explained using the same linear mechanism discussed below.

To explain these effects, consider how feedback affects the amplification of disturbances. Without control, the transfer function from disturbances to measured pressure is simply  $P(s)$  (see Figure 1). With (negative) feedback, the transfer function is  $P(s)/(1 + P(s)C(s))$ , so the open-loop transfer function is modified by the amount

$$S(s) = \frac{1}{1 + P(s)C(s)} \tag{4.1}$$

called the *sensitivity function*. If  $|S(i\omega)| < 1$ , then disturbances are attenuated, so feedback is beneficial, but if  $|S(i\omega)| > 1$ , then disturbances are amplified by control.

The sensitivity function may be determined from a Nyquist plot of the system, which is just a plot of  $P(i\omega)C(i\omega)$  in the complex plane, as  $\omega$  varies from  $0 \rightarrow \infty$ . Figure 7 shows the Nyquist plot for the plant  $P(s)$  given by the empirically tuned model shown in Figure 5, and for  $C(s)$  given by a bandpass filter, with a gain and time delay. Graphically, the magnitude of the sensitivity function  $S(i\omega)$  is the reciprocal of the distance from  $P(i\omega)C(i\omega)$  to the  $-1$  point. Thus, from Figure 7, we would expect the peak frequency of 334 Hz to be attenuated, since this point is far from the  $-1$  point, while frequencies at 320 Hz and 350 Hz should be amplified by the feedback loop, as these points on the Nyquist plot lie inside the unit circle centered about the  $-1$  point, and thus correspond to  $|S(i\omega)| > 1$ . As expected, feedback attenuates the main frequency, but amplifies sidebands.

If the gain is increased, the entire Nyquist plot is magnified, so the 334 Hz peak moves farther from the  $-1$  point, while the sidebands move closer, so the main frequency should be attenuated more, while the side peaks should be amplified more. This effect is also consistent with the observed experimental behavior.

For a slightly smaller time delay than that used in Figure 7, the Nyquist plot will

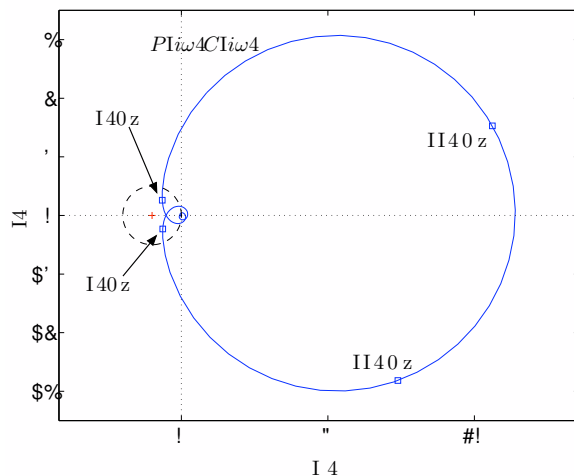


FIGURE 7. Nyquist plot for the feedback system, along with corresponding frequencies (in Hz). Points outside the dashed circle correspond to a performance benefit ( $|S(i\omega)| < 1$ ), and points inside the circle correspond to a penalty ( $|S(i\omega)| > 1$ ).

be rotated slightly counter-clockwise, so the lower frequency sideband at 320 Hz will be amplified more, while the higher frequency sideband at 350 Hz will not be amplified as much. Conversely, for a slightly larger time delay, the Nyquist plot will be rotated clockwise, so the 350 Hz sideband should be amplified more. These effects are all consistent with the experimental results shown in Figure 6.

#### 4.3. Fundamental limitations of closed-loop control

Ideally, one would like to design a compensator  $C(s)$  such that the sensitivity function  $|S(i\omega)| \ll 1$  for all frequencies. Unfortunately, this is not possible, because of *Bode's integral formula* (also known as the *area rule*), which states that under weak assumptions, any decrease in sensitivity over one frequency range must be balanced by an increase for some other frequencies (Doyle *et al.* 1992). More precisely, for a system with relative degree at least 2, the area rule states that

$$\int_0^{\infty} \log |S(i\omega)| d\omega = \pi \sum_k \operatorname{Re}(p_k), \quad (4.2)$$

where  $p_k$  are the unstable poles of  $PC$ . So for a stable plant, any negative area ( $|S(i\omega)| < 1$ ) in the log-linear plot of  $S$  versus  $\omega$  must be balanced by an equal positive area ( $|S(i\omega)| > 1$ ), no matter how the controller  $C(s)$  is chosen. For unstable plants, the situation is worse, and the net area must be positive.

The area rule in itself does not imply any peaking of  $|S(i\omega)|$ , as the positive area may be spread out over a large frequency band, as  $\omega \rightarrow \infty$ . However, Banaszuk *et al.* (2001) showed that for narrow bandwidth controllers, and plants with significant time delays, the area rule does imply a peaking of  $|S(i\omega)|$ , since all of the amplification must occur within the narrow bandwidth of the controller. The more narrow the bandwidth, or the longer the time delay, the greater the amount of peaking. This implies a strong argument in favor of large bandwidth actuators, and suggests that narrow-bandwidth actuators (such as piezoelectrics) might not be suitable for feedback control.

## 5. Conclusions

We have presented a linear model for cavity oscillations, incorporating the effect of external disturbances. Under some conditions, the system is unstable, and perturbations will grow until nonlinearities become important and the linear model is no longer valid. However, for other conditions, the system is stable, but lightly damped, acting as a noise amplifier. Phase portraits and probability density functions of experimental data indicate that for most flow regimes observed in our experiment, the cavity is a stable noise amplifier, oscillating at several different Rossiter modes. For the  $M = 0.35$  case, however, the flow is in a limit cycle, oscillating at a single Rossiter mode, probably because of enhanced acoustic resonance at this value of  $M$ .

For this Mach number, the flow may be stabilized using a controller consisting of a bandpass filter and time delay. When control is introduced, however, a peak-splitting phenomenon is observed, in which the main peak splits into two sidebands. These same effects are found in the linear model. The peak splitting effect has been observed in experiments in combustion instabilities by Banaszuk *et al.* (2001), and is a common feature of systems with limited bandwidth and large time delay.

If the noise-amplification model of cavity oscillations is correct, one cannot expect to be able to reduce the amplitude of oscillations at all frequencies using feedback, because of fundamental limitations imposed by the area rule. However, given an accurate model of the system (e.g., from a frequency response experiment), it is straightforward to design a compensator to minimize these adverse effects, and reduce oscillations over important frequency ranges, while paying the penalty over less important frequency ranges, or ranges where the plant itself is not so sensitive to disturbances.

Finally, we note that while nonlinearities may be important for cavity oscillations in other parameter ranges, the controlled system will hopefully always be stable, so the linear models presented here should always be useful to understand the controlled system.

We would like to thank Andrzej Banaszuk for many helpful comments, and for suggesting the method for distinguishing between stable and unstable noisy systems. The theoretical work was supported by AFOSR under grant F49620-98-1-0095 with program manager Dr. Thomas Beutner. The experimental work was supported by AFOSR under grant F49620-98-1-0276, with program manager Dr. Steve Walker.

## REFERENCES

- BANASZUK, A., MEHTA, P. G., JACOBSON, C. A. & Khibnik, A. I. 2001 Limits of achievable performance of controlled combustion processes. *IEEE Trans. Automat. Contr.* (submitted).
- CATTAFESTA, III, L. N., SHUKLA, D., GARG, S. & ROSS, J. A. 1999 Development of an adaptive weapons-bay suppression system. AIAA Paper 99-1901.
- CRIGHTON, D. G. 1992 The jet edge-tone feedback cycle; linear theory for the operating stages. *J. Fluid Mech.* **234**, 361–391.
- DOYLE, J. C., FRANCIS, B. A. & TANNENBAUM, A. R. 1992 *Feedback Control Theory*. Macmillan.
- HUERRE, P. & MONKEWITZ, P. A. 1990 Local and global instabilities in spatially developing flows. *Ann. Rev. Fluid Mech.* **22**, 473–537.
- KERSCHEN, E. J. & TUMIN, A. 2003 A theoretical model of cavity acoustic resonances based on edge scattering processes. AIAA Paper 2003-0175.
- MEZIĆ, I. & BANASZUK, A. 2000 Comparison of systems with complex behavior: Spectral methods. Conference on Decision and Control.
- ROSSITER, J. E. 1964 Wind-tunnel experiments on the flow over rectangular cavities at subsonic and transonic speeds. Aeronautical Research Council Reports and Memoranda, No. 3438.

- ROWLEY, C. W., COLONIUS, T. & BASU, A. J. 2002 On self-sustained oscillations in two-dimensional compressible flow over rectangular cavities. *J. Fluid Mech.* **455**, 315–346.
- SAROHIA, V. 1975 Experimental and analytical investigation of oscillations in flows over cavities. PhD thesis, California Institute of Technology.
- SMITH, B. L. & GLEZER, A. 1998 The formation and evolution of synthetic jets. *physfluids* **10** (9), 2281–2297.
- TAM, C. K. W. & BLOCK, P. J. W. 1978 On the tones and pressure oscillations induced by flow over rectangular cavities. *J. Fluid Mech.* **89** (2), 373–399.
- WILLIAMS, D. R., FABRIS, D. & MORROW, J. 2000 Experiments on controlling multiple acoustic modes in cavities. AIAA Paper 2000-1903.